

Multiple 0 - π transitions in SIFS Josephson tunnel junctions

F. Born and M. Siegel

Karlsruhe University, Institute of Micro- and Nanoelectronics Systems, Karlsruhe, Germany

E. K. Hollmann and H. Braak

Research Center Jülich, ISG and IFF, Jülich, Germany

A. A. Golubov

Faculty of Science and Technology, University of Twente, Enschede, The Netherlands

D. Yu. Guskova and M. Yu. Kupriyanov

Institute of Nuclear Physics, Moscow State University, Moscow, Russia

We report on experimental studies of superconducting coupling through a thin $\text{Ni}_{76}\text{Al}_{24}$ film. A new patterning process has been developed, which allows in combination with the wedge shaped deposition technique the in situ deposition of 20 single $\text{Nb}/\text{Al}/\text{Al}_2\text{O}_3/\text{Ni}_3\text{Al}/\text{Nb}$ multilayers, each with its own well defined Ni_3Al thickness. Every single multilayer consists of 10 different sized Josephson junctions, showing a high reproducibility and scaling with its junction area. Up to six damped oscillations of the critical current density against F-layer thickness were observed, revealing three single 0- π -transitions in the ground state of Josephson junctions. Contrary to former experimental studies, the exponential decay length is one magnitude larger than the oscillation period defining decay length. The theoretical predictions based on linearized Eilenberger equations result in excellent agreement of theory and experimental results.

PACS numbers: 74.25.Ha, 74.50.+r, 01.30.Rr

In the past few years there was a noticeable interest to the unconventional Josephson junctions [1, 2, 3], in particular, to the so-called π - junctions having negative critical current. These junctions provide a π - shift in the ground state and were realised experimentally in SFS (superconductor-ferromagnet-superconductor) and some HTS structures.

The intensive experimental study of “0” – “ π ” transition in SFS Josephson junctions [4, 5, 6, 7, 8, 9, 10, 11, 12, 13] confirms the existence of critical current oscillations upon the thickness of ferromagnetic interlayer d_f . Different structure of SFS sandwiches and SIFS tunnel junctions having been fabricated up to now. They contain regions which are controlling the critical current and difficult to control in experiment and describe in theory. They are SF interfaces, dead layers, and the region in S banks with suppressed superconductivity. Contrary to that the bulk properties of F material can be better controlled and well described by theoretical models based on quasiclassical theory of superconductivity. These theories predict that for large thickness of ferromagnet the critical current of SFS junctions have to exhibit a damped oscillations as a function of d_f

$$I_c(d_f) = I_c(d_0) \frac{\left| \sin\left(\frac{d_f - d_1}{\xi_{F2}}\right) \right|}{\left| \sin\left(\frac{d_1 - d_0}{\xi_{F2}}\right) \right|} \exp \left\{ -\frac{d_f - d_0}{\xi_{F1}} \right\}. \quad (1)$$

Here d_1 is the position of the first minima, $I_c(d_0)$ is the first experimental value of $I_c(d_f)$. These two values take into account the resultant action of SF interfaces and their vicinities. The oscillations are characterized by two

effective lengths. They are the decay length ξ_1 , and the length ξ_2 , which determines the period of oscillations. In dirty limit the expressions for $\xi_{1,2}$ follow from the Usadel equations [14] and have the form

$$\xi_{1,2} = \sqrt{\frac{D_f}{\sqrt{(\pi T)^2 + E_{ex}^2} \pm \pi T}} \quad (2)$$

where D_f and E_{ex} are the diffusive coefficient and exchange field of ferromagnetic material, respectively. In the clean limit one can easily get from Eilenberger equations that [15]

$$\xi_1^{-1} = \xi_0^{-1} + l^{-1}, \quad \xi_0 = \frac{v_F}{2\pi T}, \quad \xi_2 = \xi_H = \frac{v_F}{2E_{ex}} \quad (3)$$

where $l \gg \xi_0$ is the electron mean free path and v_F is the Fermi velocity in a ferromagnet.

It is clearly seen from Eqs. (2) and (3) that for dirty materials $\xi_2 > \xi_1$, and in the limit of large exchange energy, $E_{ex} \gg \pi T$, the characteristic lengths are nearly equal $\xi_1 \simeq \xi_2$. In the clean limit these ξ_1 and ξ_2 are completely independent.

Our analysis of both the bulk properties of ferromagnet materials [16] and the experimental data [4, 5, 6, 7, 8, 9, 10, 11, 12, 13] has shown (see Table I) that in dilute ferromagnets [5, 8, 10, 11] the electron mean free path is very small providing the fulfilment of the dirty limit conditions for the F interlayer. In these experiments $\xi_1 \simeq \xi_2$ as it follows from Eq. (2). Contrary to that, in the structures with Ni interlayer the relation between ξ_2 and ξ_1 is just the opposite so that more complex

TABLE I: Characteristic lengths in ferromagnetic materials for SFS Josephson junctions.

Ref.	$\xi_1(\text{nm})$	$\xi_2(\text{nm})$	F-material	$v_F(\text{m/s})$	$E_{ex}(\text{K})$
[8]	1.2	1.6	$\text{Fe}_{20}\text{Ni}_{80}$	$2.2 \cdot 10^5$	1100
[11]	1.8	2	$\text{Pd}_{0.9}\text{Ni}_{0.1}$	$2 \cdot 10^5$	400
[10]	1.2	3.5	$\text{Cu}_{0.53}\text{Ni}_{0.47}$		850
[5]			$\text{Cu}_{0.52}\text{Ni}_{0.48}$		
[9]	1.7	1	Ni	$2.8 \cdot 10^5$	2300
this work	4.6	0.45	Ni_3Al	$1.5 \cdot 10^5$	1000

model [17] should be used for the data interpretation. It is necessary to point out that in all previous experiments (except [13]) the structures were not fabricated in one run, so that the certain degree of non-reproducibility of magnetic constants of F materials occurred for junctions with different d_f . This results in increase of spread of data with increasing d_f and did not permit to observe the large amount of oscillations.

In this work, we improved the reproducibility of the junction parameters by preparing the structures in one run with F - layer thickness between 10 nm and 20 nm. For the first time, we succeeded in observation of up to six damped oscillations of critical current with F - layer thickness. To do this we have used the "wedge" shaped F - layer technique and a new ferromagnetic material (Ni_3Al). We experimentally obtained a one order of magnitude difference between ξ_1 and ξ_2 which is consistent with theory based on the Eilenberger equations [15].

The bottom electrode of SIFS samples consists of Nb/Al/Nb/Al and was deposited on oxidized 2 inch Si wafers with argon magnetron sputtering. The top 10 nm thick Al layer has been oxidized for 2 minutes in a 0,1 mbar pure oxygen. The following Ni_3Al interlayer was sputtered with neon gas from one single target. The target composition of the alloy was determined by Ruther-

ford Backscattering (RBS) and is $\text{Ni}_{74}\text{Al}_{26}$. A 30 nm Nb top layer was deposited in situ to prevent the inter-layer from oxidation. A schematic cross section of the deposited multilayer is shown in insert of Fig. 1. To achieve a thickness - gradient of the Ni_3Al layer the position of the target above the substrate has been shifted during deposition for several centimeter. This permits us to produce a rather linear thickness gradient over the whole 2 inch substrate (see Fig. 1).

The transport measurements were performed at 4,2 K. Figure 2 shows the dependence of the critical current, I_C , upon external magnetic field H . The rather optimal agreement between experimental results and the Fraunhofer function fit indicates a uniform and homogenous current distribution in the junction. The current-voltage characteristics (CVC) of several Josephson junctions can be seen in Fig. 3. They show a clear superconducting tunnelling behaviour with a hysteresis in its curves. These four curves belong to one defined Ni_3Al layer thickness of 12.5 nm. The current is normalized to the current density, since the four junctions differ in their sizes. It can be seen in Fig. 3, that the current density differs only several percent, thus showing a good reproducibility of our junctions. This result also indicates that within one patterned line the F - layer thickness variation could be neglected. The thickness gradient has been characterized and proofed with RBS measurements. The variations are several Angstroms. We developed a patterning process that allows the creation of 20 different separated 500 μm wide lines, distributed homogeneous along the F - layer thickness gradient over the 2 inch wafer. Each lines consists of 10 different sized circular Josephson junctions. The junction area differs from 5 to 1000 μm^2 . The variation of F - layer thickness inside an individual junction is negligible small. The ferromagnetic properties of Ni_3Al films depend on neon pressure. Details will be published elsewhere [18]. The magnetic properties of the Ni_3Al lay-

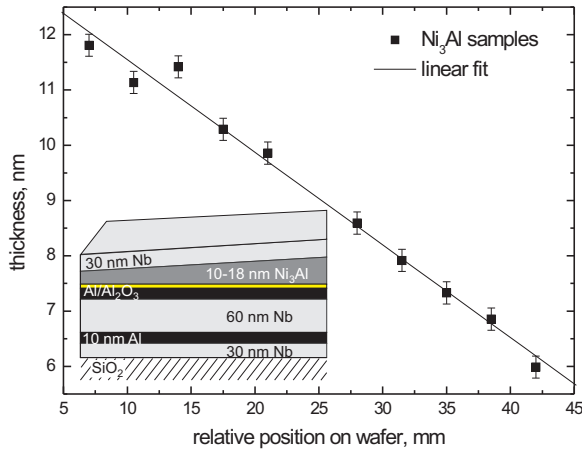


FIG. 1: $\text{Ni}_{76}\text{Al}_{24}$ film thickness measured at different positions on a 2 inch Si wafer with the RBS method. Inset: layer sequence in a cross section.

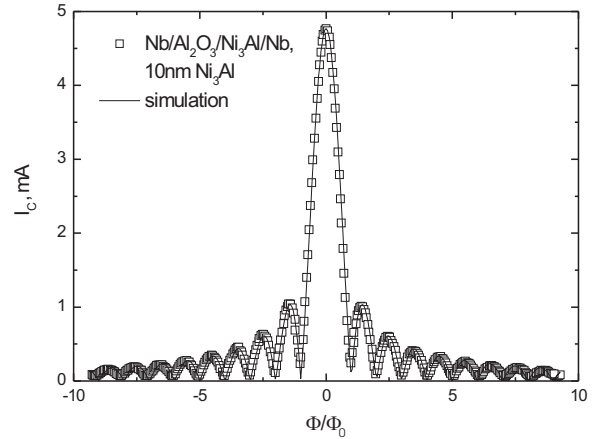


FIG. 2: Fraunhofer - pattern of a typical circular Nb/Al/Al₂O₃/Ni₃Al/Nb Josephson junction, measured at 4.2K (rectangles). The junction size is about 1000 μm^2 . The solid line results from a fit to the Fraunhofer function.

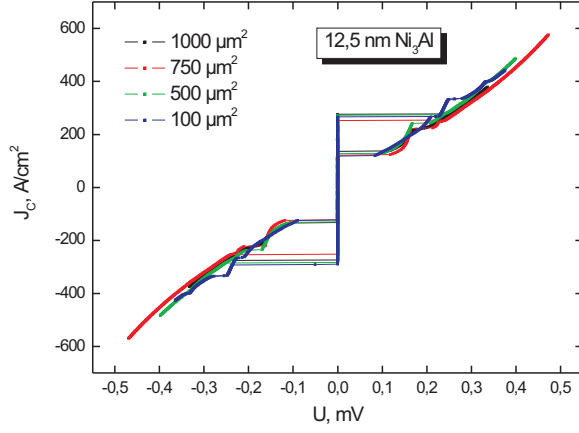


FIG. 3: Current density vs. voltage characteristics of four different Josephson junctions from one patterned line with different junction sizes, measured at 4.2 K. The size of junctions changes from $100 \mu\text{m}^2$ to $1000 \mu\text{m}^2$. The F-layer thickness is 12.5 nm.

ers were measured with a SQUID - magnetometer. The Curie temperature for a 250 nm thick Ni_3Al layer is 74 K.

The Ni_3Al thickness dependence of the critical current density can be seen in Fig. 4. Several Josephson junctions of each line were measured and plotted versus their corresponding Ni_3Al -layer thickness. A clear oscillating behavior of the critical current density of more than 60 single junctions versus d_F is shown, indicating three different $0 - \pi$ transitions. The amplitude of oscillations decays exponentially with a characteristic decay length of $\xi_1 = 4.6$ nm. It should be pointed out that the corresponding oscillation period, given by $\pi\xi_2$, is one magnitude smaller, namely $\xi_2 = 0.45$ nm. There is a rather good agreement of the theoretical fit after Eq. (1) with these two decay length's, see solid line in Fig. 4. The magnetically dead layer has been measured for different interfaces. Corresponding to this SIFS multilayer, we achieved a thickness of the dead layer around 5 nm to 8 nm for each interface. So, we expected the first oscillation period at around 10 nm or even more. To find a theoretical explanation for the large difference between ξ_1 and ξ_2 we start with linearized Eilenberger equations which are valid at the distances from SF interface larger than ξ_1

$$2f + \frac{v_f \cos \theta}{\omega + iE_{ex}} \frac{d}{dx} f = \frac{\langle f \rangle - f}{\tau(\omega + iE_{ex})}, \quad \langle () \rangle = \int_0^\pi () \sin \theta d\theta \quad (4)$$

Here θ is the angle between direction of the Fermi velocity and interface normal, $\tau = v_F/l$ is the scattering time.

The solution of this equation has the form [19]

$$f(x, \theta) = C(\theta) \exp \left\{ -\frac{x}{\xi_{eff}} \right\}, \quad \xi_{eff}^{-1} = \xi_1^{-1} + i\xi_2^{-1}, \quad (5)$$

where ξ_{eff} is the effective decay length which is independent on θ and $C(\theta)$ is an integration constant. Substitu-

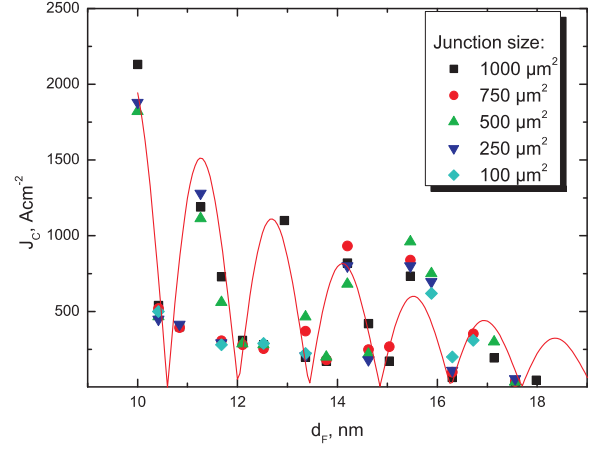


FIG. 4: Critical current density of up to 60 single SIFS Josephson junctions against the F - layer thickness. The solid line indicates a theoretical fit after Eq. (1) with the two fitting parameters $\xi_1 = 4.6$ nm and $\xi_2 = 0.45$ nm.

tion of Eq. (5) into Eq. (4) gives

$$C(\theta) = \frac{\eta \langle C \rangle}{1 - k^2 \cos^2 \theta}, \quad \eta = \frac{\ell^{-1}}{\xi_0^{-1} + \ell^{-1} + i\xi_H^{-1}}, \quad k = \frac{\eta \ell}{\xi_{eff}} \quad (6)$$

Integration of Eq. (6) over angle θ provides the equation for ξ_{eff}

$$\tanh \frac{\ell}{\xi_{eff}} = \frac{\xi_{eff}^{-1}}{\xi_0^{-1} + \ell^{-1} + i\xi_H^{-1}}. \quad (7)$$

In the dirty limit, $\ell \ll \xi_0 \xi_H (\xi_H + \sqrt{\xi_0^2 + \xi_H^2})^{-1}$ and in the clean limit $1 + \ell \xi_0^{-1} \gg \frac{1}{2} \max \{ \ln(1 + \ell \xi_0^{-1}), \ln(\ell \xi_H^{-1}) \}$, the solution of Eq. (7) reduces to Eqs. (2) and (3), respectively. The results of numerical solution of Eq. (7) are presented in Fig. 5.

There are steps on $\xi_2^{-1}(\xi_H^{-1})$ and ξ_2/ξ_1 vs ξ_H^{-1} dependencies (see Fig. 5) accompanied by the minima on $\xi_1^{-1}(\xi_H^{-1})$ curves (see Fig. 5, right inset). The ratio of ξ_2/ξ_1 falls very rapidly with increase of ξ_H . It follows from Fig. 5 that the experimental value of this ratio $\xi_2/\xi_1 \approx 0.1$ can be achieved at $l \approx 10\xi_H$. For the estimated earlier parameters $\xi_1 \approx 4.5$ nm and $\xi_2 \approx 0.5$ nm from Fig. 5, left inset and Fig. 5, right inset we get nearly equal values for the electron mean free path $l \approx 1.4\xi_1 \approx 6, 3$ nm and $l \approx 11\xi_2 \approx 5$ nm respectively. In the last estimation it was also supposed that $l/\xi_0 \approx 0.1$, resulting in $\xi_0 \approx 50$ nm and Fermi velocity $v_F = 1, 8 \cdot 10^5$ m/s. With this value of v_F and $\xi_H \approx 0.1l \approx 0.5$ nm we arrived at $E_{ex} \approx 1300$ K ≈ 0.11 eV. This combination of parameters is not unique. Starting from $l \approx 20\xi_H$ and $l/\xi_0 \approx 0.3$ one can get $l \approx 9.5$ nm, $\xi_0 \approx 30$ nm, $v_F = 1.2 \cdot 10^5$ m/s and $E_{ex} \approx 900$ K $\approx 0, 08$ eV. These parameters are consistent with the previous experimental data integrated into Table I.

The discovered behavior of ξ_2 and ξ_1 is quite general and must be also observed in structures without ferro-

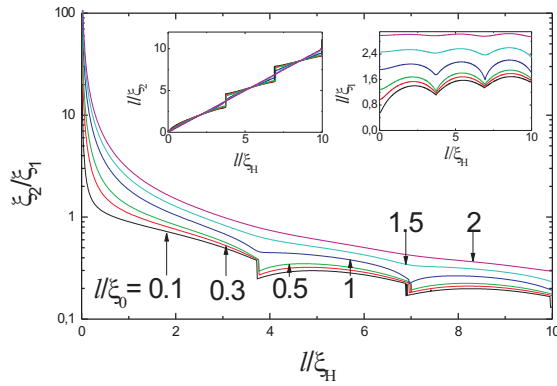


FIG. 5: Dependence of the ratio ξ_2/ξ_1 on inverse magnetic length l/ξ_H calculated for different ratios of l/ξ_0 . Left inset: Inverse decay length l/ξ_2 vs inverse magnetic length l/ξ_H for different ratios of l/ξ_0 . Right inset: Inverse decay length l/ξ_1 vs inverse magnetic length l/ξ_H for different ratios of l/ξ_0 .

magnetic ordering. An example is a normal filament of finite length, which is placed between superconducting banks and is biased by a dc supercurrent. It was shown [20], that the minigap induced to this filament from the S electrodes is not a monotonous function of phase difference across the structure. This behavior could be also explained in terms of specific dependencies of ξ_2 and ξ_1 upon electron mean free path in current biased systems.

Summarising the presented results we conclude that utilization of the new ferromagnetic material, Ni_3Al , as well as the wedge technique for its deposition permits for the first time the experimental demonstration as much as six oscillations of the critical current as a function

of thickness of ferromagnetic layer. High reproducibility of the junctions parameters, their scaling with the area, suppression of oscillation observed after only one change in operation-routing sequence, namely, replacement of Ar by Ne during the sputtering of Ni_3Al , clearly manifests that observed effect is due to magnetic ordering in Ni_3Al film. The fact of this ordering has been also confirmed by independent examination of magnetization of the Ni_3Al films. It is important also to mention that Ni_3Al is an intermetallide. This metal is widely used and well studied before [16]. It successfully combines the relatively small values of exchange integral with the transport properties close to that of strong pure ferromagnets. We believe that it will substitute the dilute ferromagnetic alloys in the SFS Josephson junction technology. The experimental results are consistent with the theoretical predictions made in the frame of the Eilenberger equations. Moreover, it was demonstrated that the intuitive knowledge about the relation between ξ_2 and ξ_1 , which is based on the dirty theories, has a very limited field of applications and can not be used for $\xi_H > 5l$ or for $E_{ex}\tau > 0.1$. In particular, it was for first time recognized that the increase of E_{ex} is not always accompanied by decrease of ξ_1 and there is some range of parameters when ξ_1 even may increase with E_{ex} . The fact that one may combine reasonably large decay length with the smaller period of oscillations looks rather attractive for possible applications of SFS Josephson junctions.

The authors thank A. D. Zaikin for useful discussions. This work was supported in part by PI-Shift Programme, RFBR grant N^o 06-02-90865 and NanoNed programme under project TCS.7029.

-
- [1] A.A. Golubov, M.Yu. Kupriyanov, E. Il'ichev, Rev.Mod.Phys. **76**, 411 (2004).
 - [2] A.I. Buzdin, Rev.Mod.Phys. **77**, 935 (2005).
 - [3] F. S. Bergeret, A. F. Volkov, and K. B. Efetov, Rev.Mod.Phys. **77**, 1321 (2005).
 - [4] V. V. Ryazanov, V. A. Oboznov, A. Y. Rusanov, *et. al.*, Phys. Rev. Lett. **86**, 2427 (2001).
 - [5] H. Sellier, C. Baraduc, F. Lefloch, *et. al.*, Phys. Rev. B **68**, 054531 (2003).
 - [6] Y. Blum, A. Tsukernik, M. Karpovski, *et. al.*, Phys. Rev. B **70**, 214501 (2004).
 - [7] C. Surgers, T. Hoss, C. Schonenberger, *et. al.*, J. Magn. Magn. Mater. **240**, 598 (2002).
 - [8] C. Bell, R. Loloee, G. Burnell, and M. G. Blamire, Phys. Rev. B **71**, 180501 (R) (2005).
 - [9] V. Shelukhin, A. Tsukernik, M. Karpovski, *et. al.*, e-print cond-mat/0512593.
 - [10] V. A. Oboznov, V.V. Bol'ginov, A. K. Feofanov, *et. al.*, e-print cond-mat/0508573.
 - [11] T. Kontos, M. Aprili, J. Lesueur, *et. al.*, Phys. Rev. Lett. **89**, 137007 (2002).
 - [12] M. Weides, K. Tillmann, and H. Kohlstedt, e-print cond-mat/0511546.
 - [13] H. Sellier, C. Baraduc, F. Lefloch, and R. Calemczuck, Phys. Rev. Lett. **92**, 257005 (2004).
 - [14] A.I. Buzdin, B. Bujicic, and M.Y. Kupriyanov, Sov.Phys. JETP **74**, 124 (1992).
 - [15] G. Eilenberger, Z. Phys. **214**, 196 (1968).
 - [16] M. Yu. Kupriyanov, A. A. Golubov, and M. Siegel, Proc. SPIE September (2006).
 - [17] F. S. Bergeret, A. F. Volkov, and K. B. Efetov, Phys. Rev. B **64**, 134506 (2001).
 - [18] F. Born, M. Siegel, E. Hollmann, H. Braak, M. Y. Kupriyanov, and V. Volpyas, submitted to Europhys. Lett. (2006).
 - [19] M. Yu. Kupriyanov, Sov. J. Low Temp. Phys. **7**, 342 (1981).
 - [20] M.V. Kalenkov, H. Kloos and A.D. Zaikin, private communication (2006).